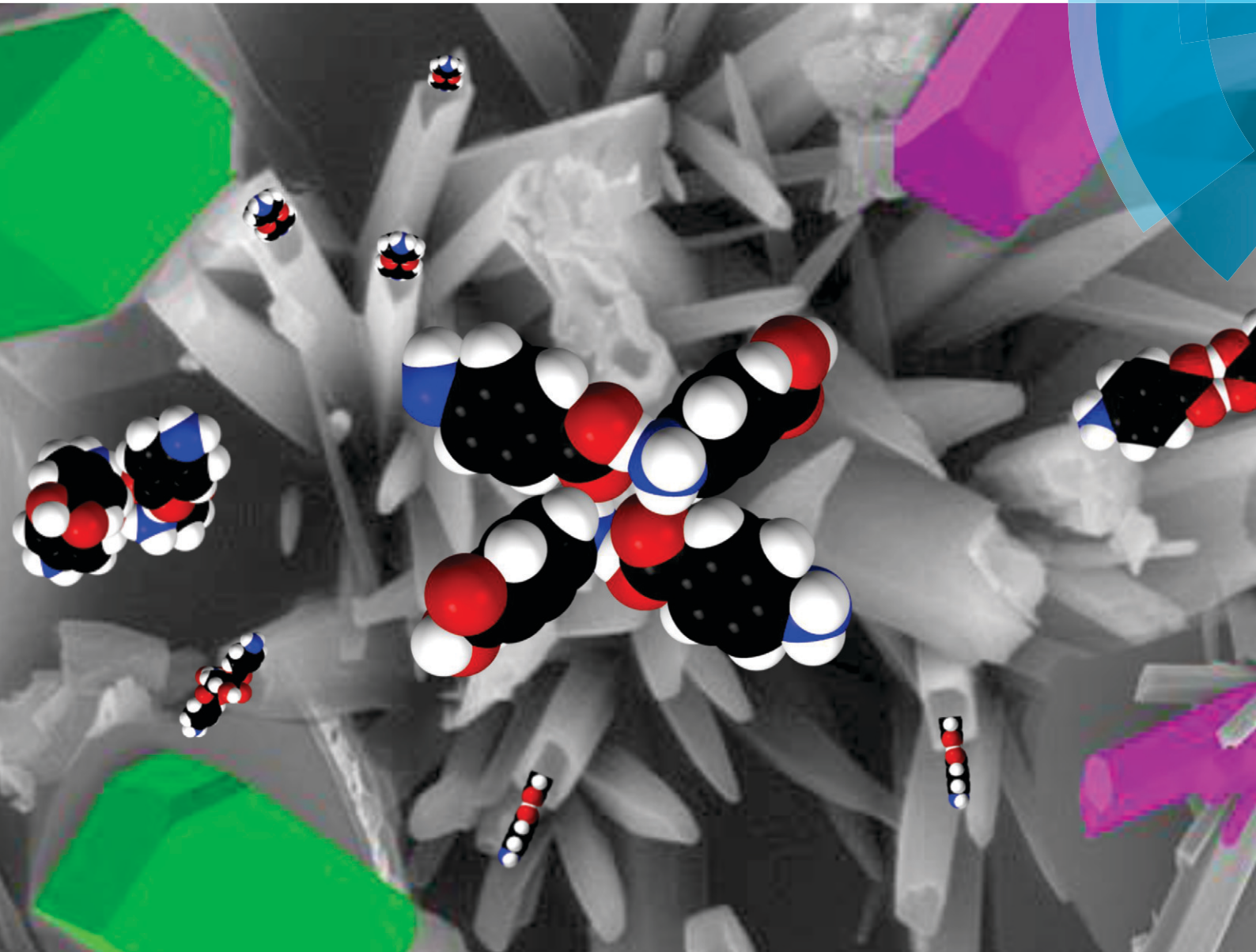


CrystEngComm

www.rsc.org/crystengcomm



PAPER

Rachel A. Sullivan and Roger J. Davey
Concerning the crystal morphologies of the α and β polymorphs of
p-aminobenzoic acid



Cite this: *CrystEngComm*, 2015, 17,
1015

Concerning the crystal morphologies of the α and β polymorphs of *p*-aminobenzoic acid[†]

Rachel A. Sullivan* and Roger J. Davey

The definition of crystal morphologies in polymorphic systems is a fundamental area of crystal engineering with implications for down-stream processing and formulation, which make morphological studies highly relevant. There are few recent examples of such detailed studies in the literature and here we address the case of *p*-aminobenzoic acid (PABA), focusing on its two polymorphic forms, α and β . Using a combination of modelling techniques to create predicted morphologies, we interpret these in the light of experimental data recorded on crystals grown from a range of polar solvents. Preliminary discussion of the intermolecular interactions involved in crystal growth of both forms, allow us to explore the enhanced morphological importance of the (002) face in α PABA and of (101) and (011) faces for β PABA. It is suggested that desolvation plays a paramount role.

Received 11th September 2014,
Accepted 23rd October 2014

DOI: 10.1039/c4ce01857e

www.rsc.org/crystengcomm

Introduction

The importance of polymorphism in the areas of solid state chemistry, process development and formulation science is well known.¹ Up until the advent of X-ray crystallography, studies of crystal morphology were routine and Groth's 1917 compilation,² based on optical methods, contains many examples of the indexed morphologies of polymorphic forms. Since then and despite the huge increase in available crystallographic data³ there have been relatively few examples in which the detailed morphologies of polymorphs have been reported. A few cases are worthy of mention: for glutamic acid the α and β forms⁴ were indexed using optical goniometry and single crystal X-ray diffraction; in the case of sulphathiazole, Blagden *et al.*⁵ used a combination of single crystal and powder XRD together with optical goniometry to index forms I to IV, while McArdle *et al.*⁶ extended this by use of morphological prediction using the HABIT program;⁷ the α , β and γ polymorphs of glycine have been the subject of numerous studies⁸ and the morphologies of all three forms are well defined. In other cases authors have been more pragmatic, for example, in the case of stearic acid, Sato and Boistelle⁹ used the overall differences in morphology to distinguish the A, B and C polymorphs, while in the case of 2,4 dihydroxybenzoic acid the morphology of form I was fully defined while the extreme fibrous nature of form II only allowed determination of the fibre direction as the *c*-axis.¹⁰ Destri *et al.*¹¹ used a combination

of morphology prediction, X-ray diffraction and optical microscopy to distinguish the three polymorphs of tolbutamide while Moreno-Calvo¹² performed a similar study on a group of monocarboxylic acids.

In the work reported here we follow the methodologies of such studies in order to describe the habits of two polymorphs, α and β of *p*-aminobenzoic acid. While there have been a number of reports of the solubility and crystallisation of these two forms from a range of solvents,^{13–15} no detailed morphological studies appear to have been made. It is known that the α form comprises *b*-axis needles¹⁶ and that β crystals are prismatic or plate-like.^{15,17} Groth includes the (pre-XRD) morphology of one of the forms (unidentified) in his compilation (ref. 2, vol. IV, p. 509). In this current work we utilise a combination of BFDH (Mercury¹⁸) and attachment energy prediction (Materials Studio¹⁹) to create predicted morphologies starting from the two ref codes AMBNAC07 (α) and AMBNAC08 (β). These are then combined with optical and SEM micrographs, pXRD of oriented samples and optical goniometry (using MORANG²⁰ to calculate angles) in order to create a more detailed picture of the morphologies of the two forms. We return to Groth's entry and attempt to establish which polymorph it is. Finally the surface chemistries of major faces are discussed in the light of crystal growth processes.

The crystal structures of the α and β polymorphs have been discussed previously.^{13,14,16,17} α PABA is made up of hydrogen bonded chains of carboxylic acid R₂²(8) dimers that pack along the *b*-axis through π – π interactions. β PABA comprises a hydrogen bonded tetramer linking alternate carboxyl and amine functional groups. These two forms are enantiotropically related with a transition temperature of 13.8 °C.¹⁵

School of Chemical Engineering and Analytical Science, The University of Manchester, Manchester M13 9PL, UK. E-mail: rachel.sullivan@manchester.ac.uk

† CCDC 983121 and 983122. For crystallographic data in CIF or other electronic format see DOI: 10.1039/c4ce01857e

More recently Benali-Cherif *et al.*²¹ have reported a non-centrosymmetric polymorph based on the two distinct carboxylic acid dimers featured in α PABA, however this form seems to appear under extreme pH conditions and is not considered in this current work.

Experimental

Growth of crystals

PABA ($\geq 99\%$) (supplied as the α form), acetonitrile ($\geq 99.5\%$), 2-propanol (anhydrous 99.5%), ethyl acetate ($\geq 99.5\%$), methanol ($\geq 99.9\%$), ethanol ($\geq 99.9\%$), nitromethane ($\geq 95.0\%$) and toluene ($\geq 99.9\%$) were purchased from Sigma Aldrich. All chemicals were used without further purification. De-ionized water was used throughout.

Single crystals of α and β PABA were grown by slow solvent evaporation at room temperature (*ca.* 25 °C). Solutions for these crystallisation experiments were prepared by making slurries of α PABA in de-ionized water, 2-propanol, ethanol, methanol, ethyl acetate, acetonitrile, nitromethane and 1 : 1 methanol : toluene at room temperature and left stirring for 4 hours. The residual solids were then allowed to settle for approximately 1 hour and 2 mL aliquots of each saturated solution were withdrawn and placed in glass vials with lids punctured in the centre only. These samples were left for up to two weeks to allow crystallisation to occur.

Microscopy

A Zeiss Axioplan 2 polarising microscope with Linksy software²² was used to capture and edit optical images. In addition, single crystals of both forms of PABA were examined using an FEI Quanta 200 ESEM, operating at high vacuum (20 kV). Samples were gold coated prior to examination.

Single crystal X-ray diffraction (SCXRD)

The crystal structures of both polymorphs (α -AMBNAC07 & β -AMBNAC08) were re-determined at 100 K on an Oxford Xcaliber 2 diffractometer, using Mo K α radiation with a graphite monochromator. Data were collected and processed using the CrysAlisPro software,²³ and the structures solved using the OLEX2 (ref. 24) program as an interface together with the SHELXS and SHELXL programs.²⁵ Heavy atoms were refined anisotropically. Hydrogen atoms were placed in geometric positions and refined as riding atoms, except for those bound to nitrogen and oxygen, which were refined freely.

Crystal morphology

In order to determine the crystal morphology of the two forms a number of complementary techniques and calculations were employed:

A STOE optical two circle goniometer (model J) was used to measure the interfacial angles of a series of single crystals of α PABA grown in both methanol and ethanol and mounted with their needle axes parallel to the goniometer axis.

Powder X-ray diffraction was employed to characterize the preferred orientation of each form. A Rigaku Miniflex benchtop machine in the Bragg–Brentano geometry was used, with all samples scanned between 5° and 40° 2 θ at a rate of 1.5° per minute and a step size of 0.03°. Samples of unground crystals, taken from each growth solvent used, were loaded into the sample holder. In the case of the α form, a group of needles were aligned roughly parallel, while for β , a number of prismatic crystals were placed adjacent to each other.

Mercury CSD 3.3© (ref. 18) was employed to visualise crystal structures and calculate the BFDH morphologies of each form. From these the Morang software²⁰ was used to calculate the interfacial angles between the major faces in order to interpret the optical goniometry data.

Further morphological calculations and optimisations were performed in Materials Studio¹⁹ using a Dreiding force field with Gasteiger charges. These calculated growth morphologies could be manipulated in order to reproduce those observed in the optical and SEM micrographs.

Results

Crystal structures

The single crystal structures of both forms were successfully re-determined and submitted to the CCDC²⁶ and are available as ref. codes AMBNAC07 and 08. These essentially confirm the earlier solutions of Lai and Marsh¹⁶ (AMBNAC01) for α and Gracine and Fischer¹⁷ (AMBNAC04) for β . It is noted that compared to the 2007 solution of the α structure (AMBNAC06) from Athimoolam,²⁷ which shows the amino group as planar, our new solution matches much more closely the Lai and Marsh 1967 structure with its more acceptable pyramidal nitrogen.²⁸

BFDH morphologies

As an appropriate starting point for exploring the morphologies of the PABA polymorphs; the equilibrium forms calculated using the BFDH approach are shown in Fig. 1.

For α PABA, although, as anticipated, elongation along the *b*-axis is suggested this is not as extreme as found experimentally where needle aspect ratios between 15 and 10⁶ have been reported.²⁹ The dominant faces in the [010] zone are (101), (10̄1), (10̄1), (101). The (002) and (00̄2) faces are far less prevalent, having minute significance in the overall calculated morphology. The end faces of the needle are (011), (110), (110), (01̄1), (11̄1) and (11̄1), and their symmetry related equivalents.

For β PABA a more equant, prismatic morphology is predicted with major faces (011), (101) and (002). This seems to compare well with the form reported by Groth² and observed by Gracine and Rasmussen,¹³ as well as the plate like hexagons of Hao *et al.*¹⁵

Experimental crystal morphologies

The crystallisation technique used yielded single crystals of α PABA from all the solvents apart from water, which was the only solvent to give β PABA.

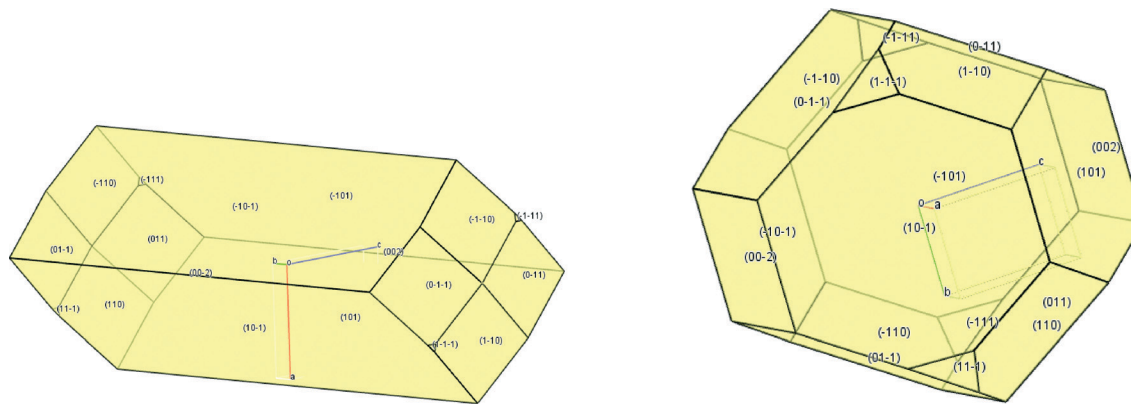


Fig. 1 BFDH morphology calculations of α PABA (left) and β PABA (right).

Preferred orientation

In order to make some preliminary and unambiguous assignment of the crystal faces, Fig. 2 compares the measured and calculated pXRD patterns of the two forms. It is apparent that as expected of *b*-axis needles, the α sample only yields diffraction peaks corresponding to planes in the (h0l) zone. In the particular example shown the –(002), (400), (006) and (008) reflections are present with all others missing. While the exact indices of the (h0l) peaks present did vary from sample to sample, in all cases (from all solvents) strong (002) reflections were observed, suggesting a much greater morphological importance of the (002) faces than indicated by the BFDH calculation.

β Crystals lay in the holder so that the X-rays essentially sampled only the large face shown in Fig. 3F. Only one diffraction peak was observed, identifying this plane as (101), one of the largest facets in the BFDH prediction. Interestingly, the BFDH prediction viewed orthogonal to this face presents a hexagonal outline very similar to the images (their Fig. 3) of Hao *et al.*¹⁵

Microscopic observations

Fig. 3A–F shows a selection of optical micrographs of crystals grown from the different solvents. In all cases the α morphologies are needle-like. In many cases, however it would appear that the crystals have a hexagonal cross section suggesting that the relative importance of (002) and (101) may not be in agreement with the BFDH prediction. It is noted that well-formed, optically clear crystals of α are difficult to grow, due largely to its tendency to fracture and twin. This behaviour, as reported earlier¹⁶ is most likely due to the creation of a pseudo mirror plane perpendicular to the *b*-axis as a result of random uptake of the $-\text{N}-\text{H}\cdots\text{O}-$ hydrogen bond. Fig. 4 shows a typical selection of microscope images of crystals which are intergrown (A and B), and fractured (B and D). Also included in this Figure (4C) is an example of needles with hollow cores, also partially evident in Fig. 3E. Overall, this growth behaviour is most apparent from aqueous solution, where not only are the needles highly anisotropic, but also tend to grow in bunches with hollow cores, possibly due

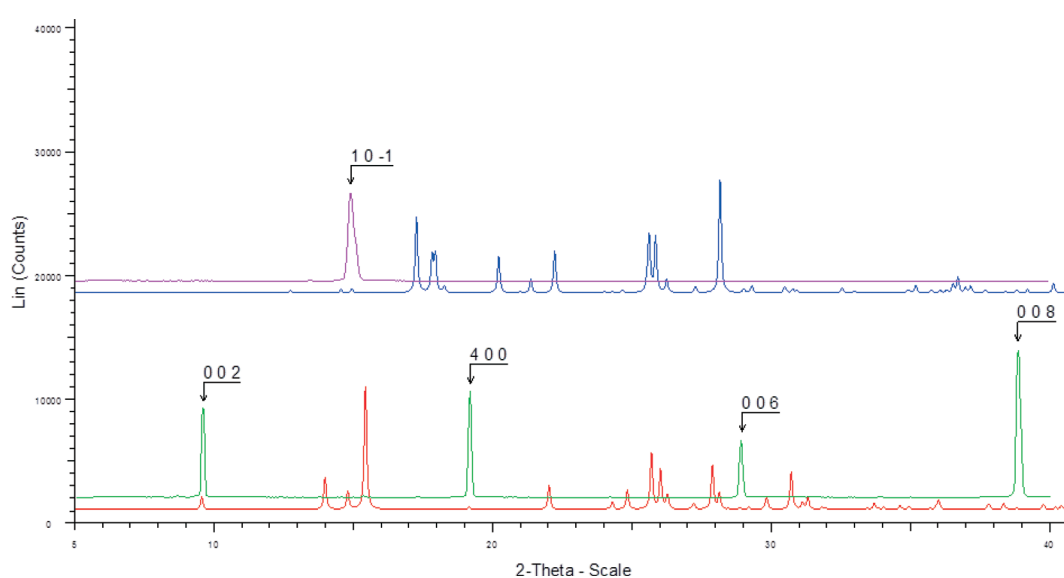


Fig. 2 Powder patterns of calculated α PABA (AMBNA07) in red; preferred orientation of α PABA crystals grown in acetonitrile in green; calculated β PABA (AMBNA08) in blue; preferred orientation of β PABA crystals grown in water in purple.

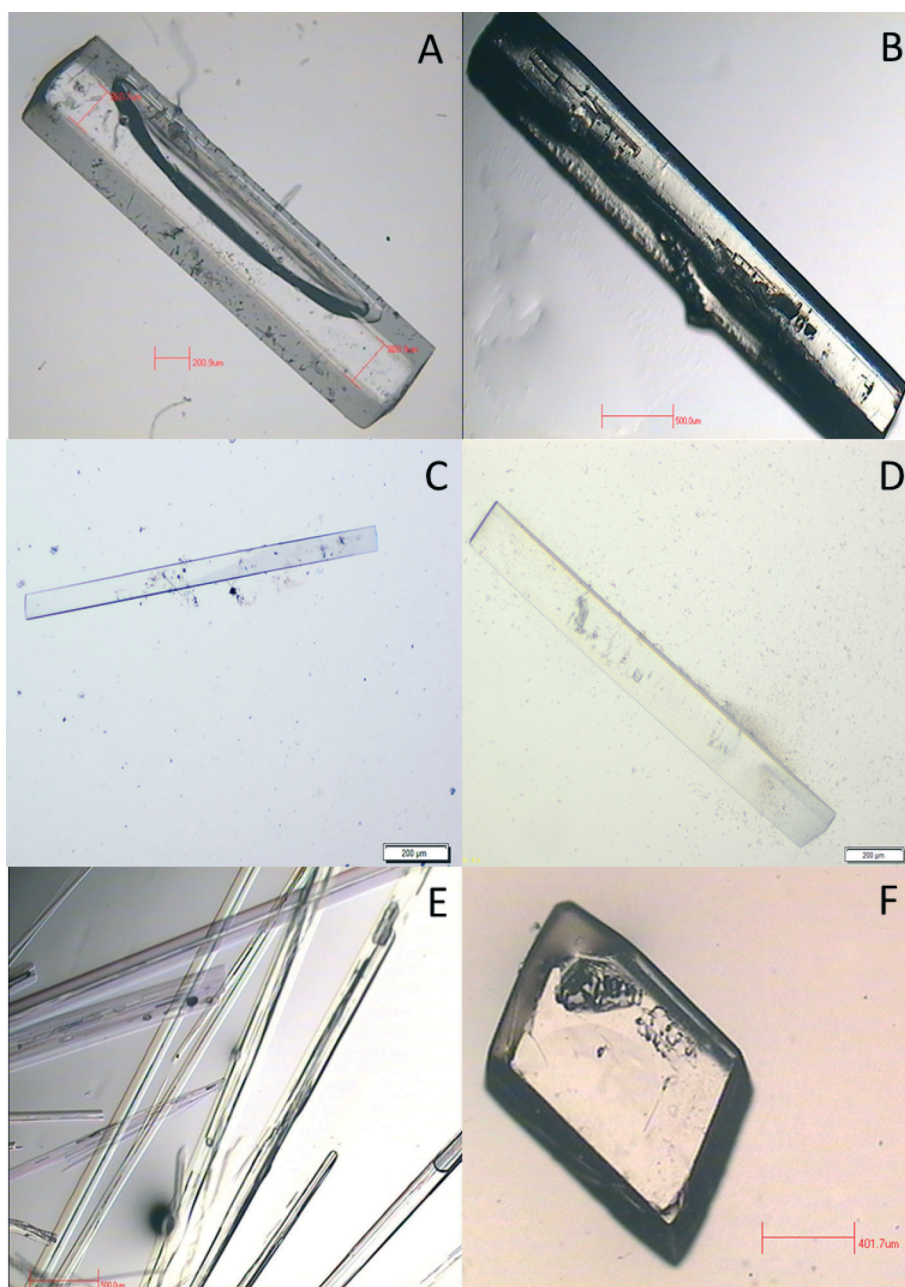


Fig. 3 Optical micrographs of samples of α PABA grown from (A) methanol (B) 2-propanol (C) acetonitrile (D) ethyl acetate (E) water and (F) β PABA grown from water.

to rapid mass transfer. Similar hollow morphologies have been reported for the growth of D,L alanine from water-IPA mixtures.³⁰ The best crystals of α were grown from alcohols.

In the case of β crystals the observed morphology of Fig. 3F is, as discussed above from previous reports, similar to that predicted by BFDH with the large face ($10\bar{1}$).

Details of these forms may be elaborated further from the SEM images of Fig. 5. Again in the case of α , the relative morphological importance of faces in the [010] zone is highlighted (Fig. 5A and B). The termination of the needles (Fig. 5C and D) is clearly variable and does not match the BFDH prediction as discussed above.

For the β form (Fig. 5E and F), the well-formed prismatic nature of the crystals is well expressed, and at least superficially are as expected from BFDH.

Optical goniometry

Due to difficulties with crystal growth of α PABA, it was found that most crystals did not present complete sets of well reflecting faces in the [010] zone. However, for four crystals (two grown from methanol and two from ethanol) it was possible to measure the interfacial angles $90 \pm 4^\circ$; $47 \pm 1^\circ$ and $43 \pm 2^\circ$ in the [010] zone. These compare well with the

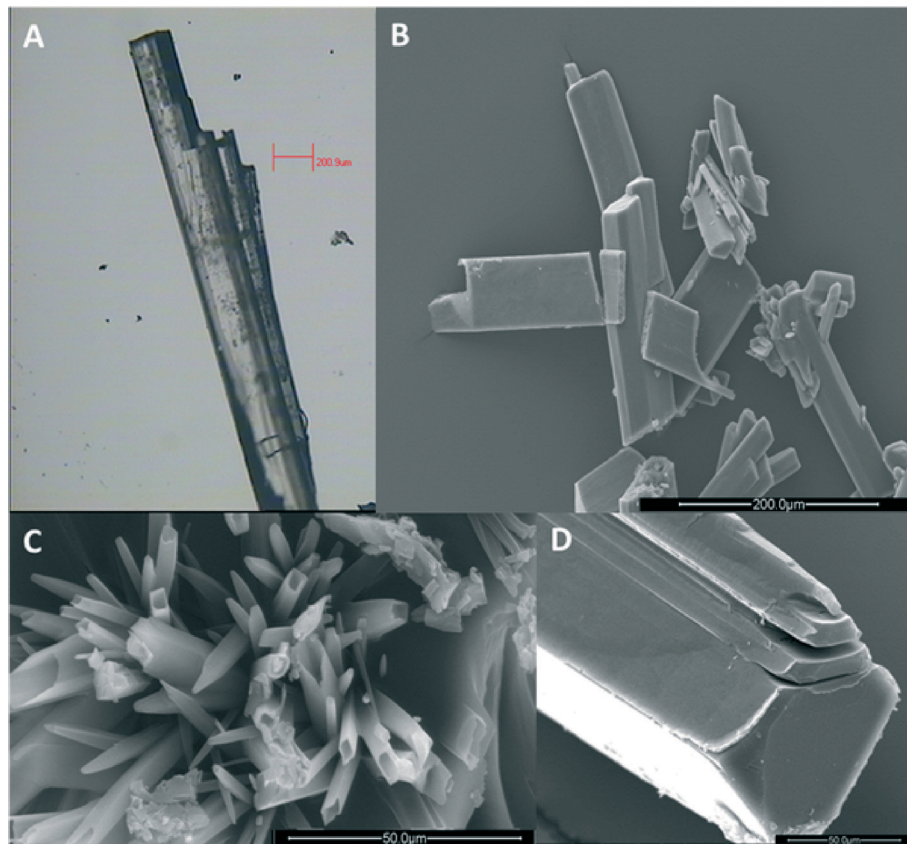


Fig. 4 Micrographs of α PABA crystals grown by slow solvent evaporation in (A) ethanol (optical micrograph), (B) nitromethane (SEM), (C) ethyl acetate (SEM), (D) acetonitrile (SEM).

computed angles (Morang) of 90.3, 46.9 and 43.3° between the $(10\bar{1})^\wedge(\bar{1}0\bar{1})$, the $(10\bar{1})^\wedge(00\bar{2})$ and the $(10\bar{1})^\wedge(002)$ faces respectively. This effectively confirms the BFDH morphology but with increased morphological importance of the $\{002\}$ faces as implied also from the pXRD and microscopy results.

The more equant morphology of β and the small crystal sizes available ruled out optical goniometry in this study. However considering the calculated angles between faces (chosen on the basis of the BFDH prediction) $(10\bar{1})^\wedge(10\bar{1})$, $(00\bar{2})^\wedge(10\bar{1})$, $(01\bar{1})^\wedge(\bar{1}0\bar{1})$ and $(01\bar{1})^\wedge(110)$ being 53.4, 55.2, 66.7 and 70.8° and comparing with Groth's table² it is apparent that many of his reported experimental values (typically 53.4, 55.9, 55.0, 55.3, 55.9, 66.8, 67.0, 70.8, 71.4, 71.6°) appear to be in agreement with the β morphology. Further to this, and given the identification of the major face by pXRD as $(10\bar{1})$, it was also possible to take the micrograph of Hao *et al.*¹⁵ (their Fig. 3) for a crystal grown from a solution mediated transformation in ethanol and measure the interior angles of the projected hexagonal microscope image. Values of approx 115, 125 and 120° were found for two of their crystals. These match well the values of 110, 120 and 125 for angles measured from the projected BFDH image viewed orthogonal to the $(10\bar{1})$ facet. This suggests that from both water and ethanol the major face remains $(10\bar{1})$ but is of increased morphological importance in ethanol.

Materials studio

The Materials Studio attachment energy morphology was not used as a means of attempting an accurate prediction of observed morphologies but rather as a tool to change the relative growth rates of faces in attempts to create diagrammatic representations which match the observed forms was performed manually after the calculation. This was taken as a further test of the consistency of our face indexing.

Thus Fig. 6A and B shows the starting morphologies calculated using the attachment energy methodology. Compared to BFDH it is noted that the $\alpha \{002\}$ and $\beta \{10\bar{1}\}$ faces have increased morphological importance. In Fig. 6C and F new morphologies have been created by modifying the relative rates of growth of the existing crystal faces. Thus, for example, for α it is possible to obtain a morphology that resembles the experimental one by increasing the importance (*i.e.* reducing the relative growth rate) of the $\{002\}$ side faces and $\{110\}$ end faces. This yields a form which matches the experimental morphology of Fig. 6D. We note that, although many α crystals appeared to be terminated (see Fig. 4A, D and 5C) by flat ends, suggesting the presence of such $\{010\}$ faces, these facets come, energetically, very far down the list (number 41) of possible growth forms calculated by Materials Studio and hence we could not force them to appear by adjustments to Fig. 6A. This point is discussed later.

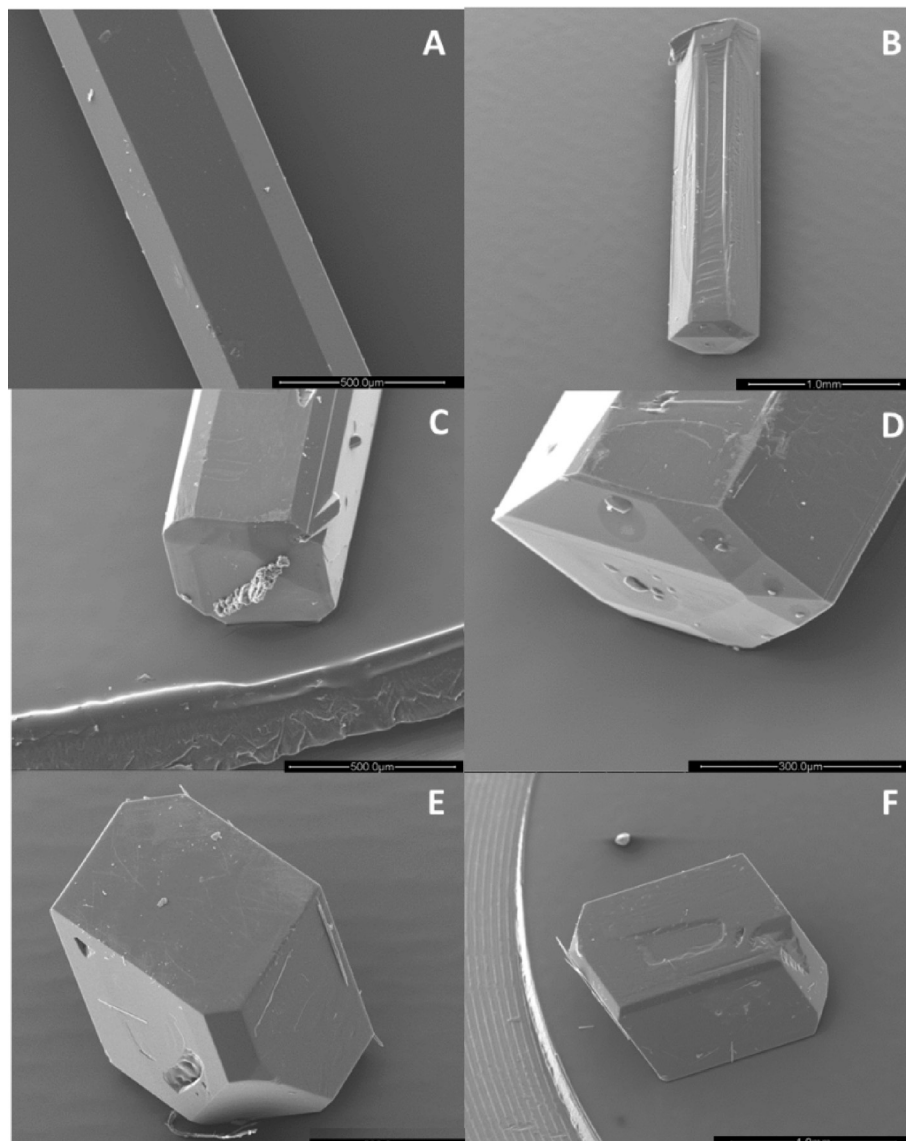


Fig. 5 SEM images of α PABA grown by slow solvent evaporation in (A) methanol (B) ethanol (C) ethyl acetate (D) ethanol and β PABA (E) & (F) water.

For β PABA, Fig. 6F was created by increasing the morphological importance of the $\{0\bar{1}\}$ faces yielding a form very close to the SEM image of Fig. 6E.

Discussion and conclusions

Here we have shown how a number of complementary experimental and computational techniques may be used to gain insight into the morphology of crystal forms in a polymorphic system. By comparing the observed experimental morphologies with the predicted ones it is possible to explore those factors, other than the structural, which might play a role in determining the morphologies. Thus, for example, in the case of α PABA it is of interest to appreciate why the $\{002\}$ faces have higher morphological importance than expected and whether $\{010\}$ might in some situations grow slowly enough to appear as the termination of the needles.

In the case of β the questions may be posed as to why $(\bar{1}01)$ might be slow growing in ethanol to yield plates and why in water (011) grows more slowly than expected.

Fig. 7 shows the packing of three relevant crystal surfaces for each form and illustrates the significant intermolecular interactions that are utilised in crystal growth. Previous work on the nucleation³¹ of α PABA showed that desolvation of the carboxylic acid group was the rate controlling step in the growth of clusters. Furthermore, earlier studies on *R,S* alanine³² showed how switching from water to ethanol changed the slowest growth direction from the amino rich to the carboxylate rich ends of the *c*-axis, again pointing to the importance of desolvation. Both of these results suggest that desolvation of the acid group should be expected to play a major role in the growth of these polymorphs. Considering firstly α PABA, the (010) face (Fig. 7) evidently cuts through the acid dimer whilst at the same time benefiting from the

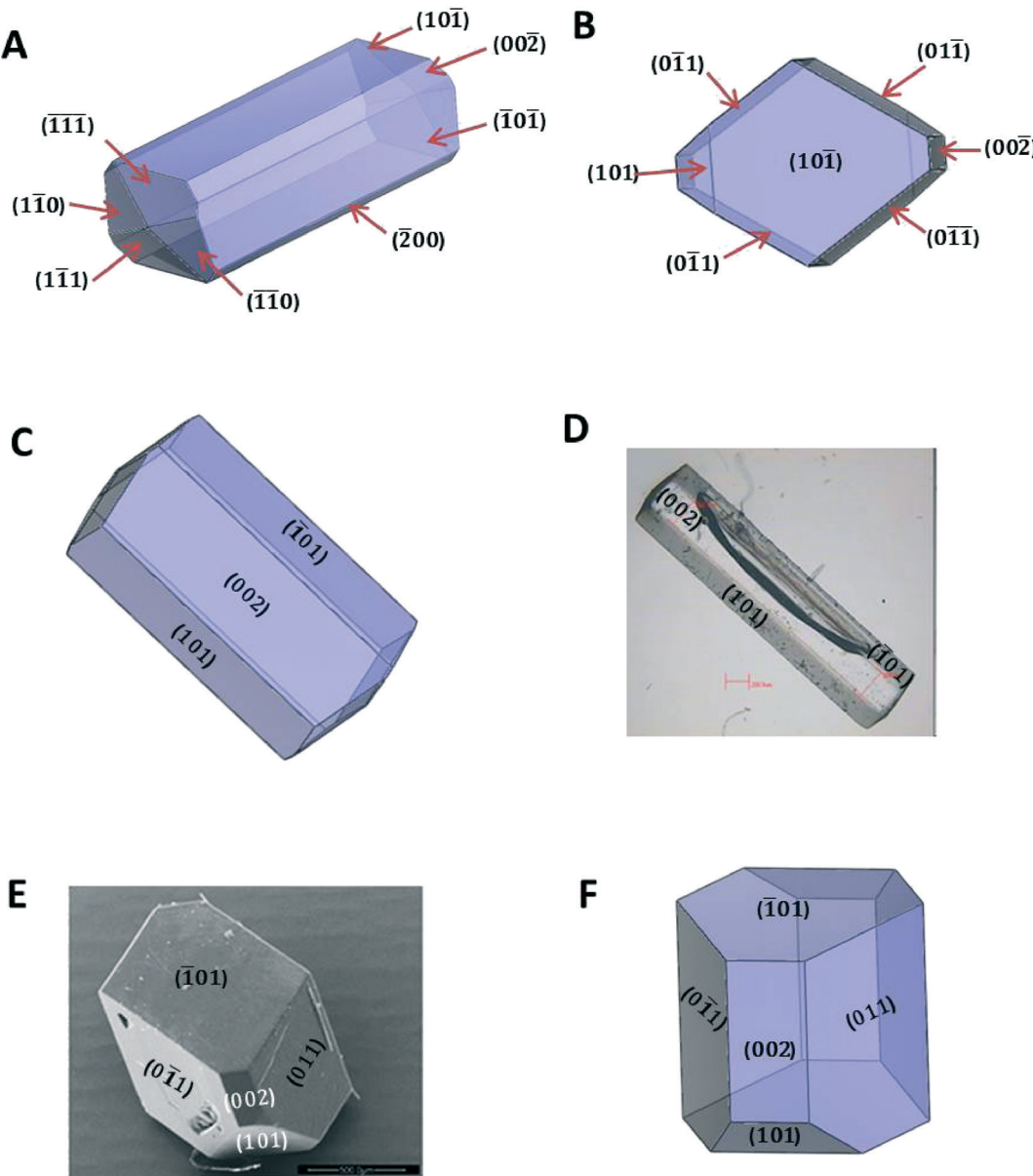


Fig. 6 Calculated versus experimental morphologies. A and B are initial calculated growth morphologies; C and D are the modified and experimental morphologies of α PABA; E and F are experimental and modified morphologies of β PABA.

$\pi\text{-}\pi$ stacking along the b -axis. The need to desolvate both the surface and the arriving acid group could well slow this face down sufficiently that it could compete with (110) as a terminating surface. The same is true for the (002) face and this need for desolvation may again be responsible for its enhanced importance. For the (101) face the acid dimer lies almost in the plane of the surface and in fact growth of this face is dominated by $\text{N-H}\cdots\text{O}$ - hydrogen bond formation and its tendency to randomise, creating the strain and twinning referred to earlier.

As far as the β form is concerned growth of the major (101) face involves completion of hydrogen-bonded tetramer and hence desolvation of both the amine and acid functionalities. Both water and ethanol seem likely to offer strong solvation

of these groups and it may be that it is the added steric barrier offered by ethanol that reduces the growth of this face sufficiently to create the plates of Hao *et al.*¹⁵ Similar arguments apply to the increased importance of (011) with this face again being important in the completion of the hydrogen bonded tetramer. Interestingly, for the (101) face the intermolecular interactions evidently lie in the plane of face so that perhaps desolvation is less crucial and the computations predict essentially the correct importance for this facet.

Overall it is evident that the observed growth morphologies of these polymorphs support our previous conclusions concerning the important role played by desolvation in determining the molecular collision frequency during nucleation.

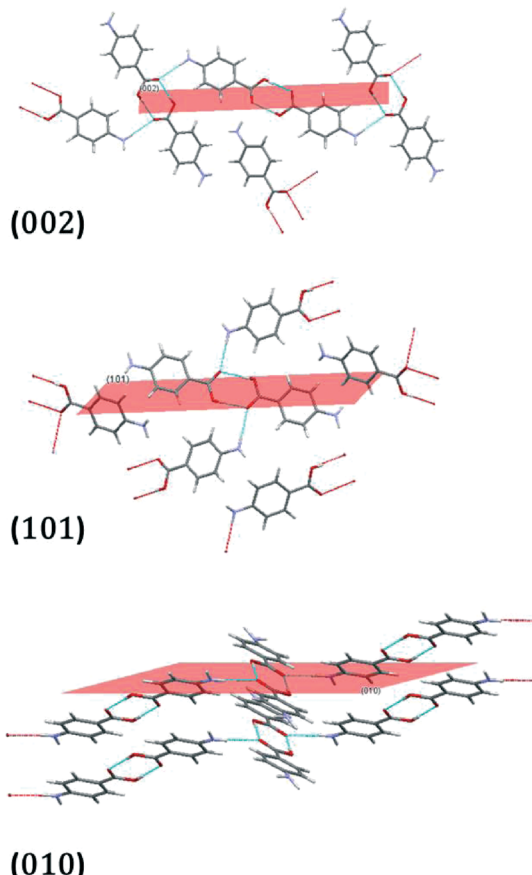
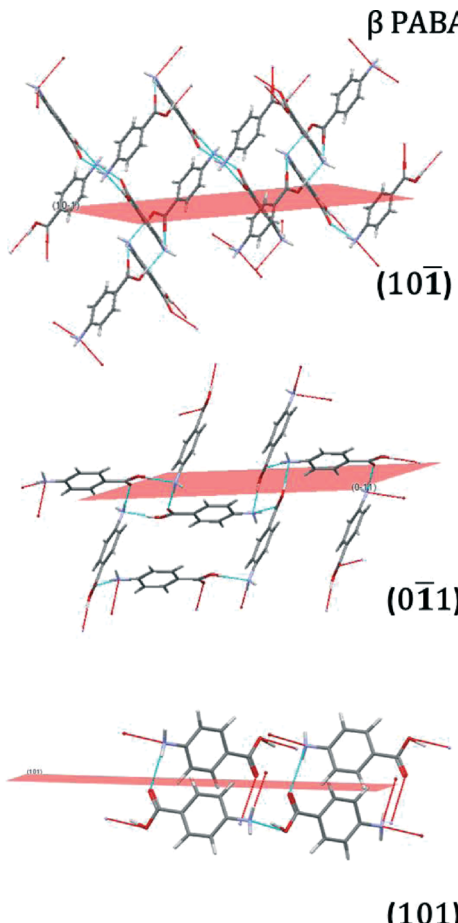
α PABA **β PABA**

Fig. 7 Intermolecular interactions in α PABA at (002), (101) and (010) faces and in β PABA at (10 $\bar{1}$), (0 $\bar{1}$ 1) and (101).

Acknowledgements

The authors wish to thank Paddy Hill for SEM images, Ian Rosbottom and Kevin Roberts of Leeds University for helpful discussions and EPSRC for funding.

References

- R. J. Davey, *Chem. Commun.*, 2003, 1463–1467.
- P. Groth, *Chemisches Kristallographie*, Engelmann, Leipzig, 1917.
- J. Bernstein, *Polymorphism in Molecular Crystals*, Clarendon Press, Oxford, 2002.
- R. J. Davey, N. Blagden, G. Potts and R. Docherty, *J. Am. Chem. Soc.*, 1997, **119**, 1767–1772.
- N. Blagden, R. J. Davey, H. F. Lieberman, L. Williams, R. Payne, R. Roberts, R. Rowe and R. Docherty, *J. Chem. Soc., Faraday Trans.*, 1998, **94**, 1035–1044.
- P. McArdle, Y. Hu, A. Lyons and R. Dark, *CrystEngComm*, 2010, **12**, 3119–3125.
- R. Docherty, G. Clydesdale, K. J. Roberts and P. Bennema, *J. Phys. D: Appl. Phys.*, 1991, **24**, 89–99.
- I. Weissbuch, V. Y. Torbeev, L. Leiserowitz and M. Lahav, *Angew. Chem., Int. Ed.*, 2005, **44**, 3226–3229.
- K. Sato and R. Boistelle, *J. Colloid Interface Sci.*, 1983, **94**, 593–596.
- R. J. Davey, N. Blagden, S. Righini, H. Alison, M. J. Quayle and S. Fuller, *Cryst. Growth Des.*, 2001, **1**, 59–65.
- G. L. Destri, A. Marrazzo, A. Rescifina and F. Punzo, *J. Pharm. Sci.*, 2013, **102**, 73–83.
- E. Moreno-Calvo, T. Calvet, M. A. Cuevas-Diarte and D. Aquilano, *Cryst. Growth Des.*, 2010, **10**, 4262–4271.
- S. Gracin and Å. C. Rasmussen, *Cryst. Growth Des.*, 2004, **4**, 1013–1023.
- M. Svard, F. L. Nordstrom, E. Hoffmann, B. Aziza and Å. C. Rasmussen, *CrystEngComm*, 2013, **15**, 5020–5031.
- H. Hao, M. Barrett, Y. Hu, W. Su, S. Ferguson, B. Wood and B. Glennon, *Org. Process Res. Dev.*, 2012, **16**, 35–41.
- T. F. Lai and R. E. Marsh, *Acta Crystallogr.*, 1967, **22**, 885–893.
- S. Gracin and A. Fischer, *Acta Crystallogr., Sect. E: Struct. Rep. Online*, 2005, **61**, 1242–1244.
- C. F. Macrae, I. J. Bruno, J. A. Chisholm, P. R. Edgington, P. McCabe, E. Pidcock, L. Rodriguez-Monge, R. Taylor, J. van de Streek and P. A. Wood, *J. Appl. Crystallogr.*, 2008, **41**, 466–470.
- Materials Studio, v 7.0.100, © 2013, Accelrys Software Inc. All rights reserved.
- R. Docherty and K. J. Roberts, *Comput. Phys. Commun.*, 1988, **51**, 423–430.

- 21 R. Benali-Cherif, R. Takouachet, E. Bendeif and N. Benali-Cherif, *Acta Crystallogr., Sect. C: Cryst. Struct. Commun.*, 2014, **70**, 323–325.
- 22 *Linksy32 software*, v 1.8.0, <http://www.linkam.co.uk/system-control-software/>.
- 23 *CrysAlis PRO*, Agilent Technologies UK Ltd, Yarnton, England, Agilent 2011.
- 24 O. V. Dolomanov, L. J. Bourhis, R. J. Gildea, J. A. K. Howard and H. Puschmann, *J. Appl. Crystallogr.*, 2009, **42**, 339–341.
- 25 G. Sheldrick, *Acta Crystallogr., Sect. A: Found. Crystallogr.*, 2008, **64**, 112–122.
- 26 F. H. Allen, *Acta Crystallogr., Sect. B: Struct. Sci.*, 2002, **58**, 380–388.
- 27 S. Athimoolam and S. Natarajan, *Acta Crystallogr., Sect. C: Cryst. Struct. Commun.*, 2007, **63**, 514–517.
- 28 J. S. Stevens, C. R. Seabourne, C. Jaye, D. A. Fischer, A. J. Scott and S. L. M. Schroeder, *J. Phys. Chem. B*, 2014, **118**, 12121–12129.
- 29 M. A. Lovette and M. F. Doherty, *Cryst. Growth Des.*, 2013, **13**, 3341–3352.
- 30 D. D. Medina and Y. Mastai, *Cryst. Growth Des.*, 2008, **8**, 3646–3651.
- 31 R. A. Sullivan, R. J. Davey, G. Sadiq, G. Dent, K. R. Back, J. H. ter Horst, D. Toroz and R. B. Hammond, *Cryst. Growth Des.*, 2014, **14**, 2689–2696.
- 32 L. J. W. Shimon, M. Vaida, L. Addadi, M. Lahav and L. Leiserowitz, *J. Am. Chem. Soc.*, 1990, **112**, 6215–6220.